Multimodal Assessment of Brain Fluid Clearance Predicts Amyloid-beta Deposition in Humans

Liangdong Zhou[1†], Tracy A. Butler[1†], Xiuyuan H. Wang[1], Ke Xi[1], Emily B. Tanzi[1], Lidia Glodzik[1], Gloria C. Chiang[1], Mony de Leon[1], Yi Li[1]

[†]**These authors contributed equally to this work.**

Abstract

Purpose: To investigate if glymphatic clearance function assessed by multimodality imaging can improve the prediction of brain beta amyloid deposition.

Methods: Two brain CSF clearance measurements (vCSF and DTI-ALPS) were derived from dynamic PET and MR diffusion tensor imaging (DTI) for 50 subjects, of which 24 were Aβ positive. T1W, T2W, DTI, T2FLAIR, and 11C-PiB and 18F-MK-6240 PET were also acquired. Multivariate linear regression models were assessed with both vCSF and DTI-ALPS as independent variables to predict the brain Aβ. Three types of models were evaluated, including vCSF model (only vCSF as clearance measure in the model), ALPS model (only ALPS as clearance measure in the model) and vCSF+ALPS model (both vCSF and ALPS, as well as their interaction term in the model). The models were applied on both the whole group and the Aβ positive group. And all the analysis were controlled for age, gender, and the intracranial volume.

Results: The mean age of finalized 50 subjects is 69.30 (sd=8.55), with male/female ratio 20/30. Our results showed that the combination of vCSF and ALPS can better predict Aβ deposit ($p < 0.05$, $R^2 = 0.575$) than each of vCSF ($p < 0.05$, $R^2 = 0.431$) or ALPS ($p < 0.05$, $R^2 = 0.372$) in Aβ positive group. the similar results has been observed in whole group (combined model: $p < 0.05$, $R^2 = 0.287$; vCSF model: $p < 0.05$, $R^2 = 0.175$; ALPS model: $p < 0.05$, $R^2 = 0.196$) with weaker effect.

Conclusion: The regression model with both vCSF and DTI-ALPS can better predict brain Aβ. Our data also showed that two independent brain clearance measurements, vCSF and DTI-ALPS, could explain more variance of Aβ deposits than each of them individually. This could

be indicative of that vCSF and DTI-ALPS reflect complementary aspects of brain clearance function.

Author affiliations:

1 Department of Radiology, Weill Cornell Medicine, New York, NY, USA

Correspondence to: Yi Li, PhD

407 E 61st St, Feil 2,

New York NY 10065,

United States

E-mail: yil4008@med.cornell.edu

Running title: Combined Clearance Biomarkers to Predict Aβ

Keywords: DTI-ALPS, vCSF slope, brain clearance, Alzheimer's disease, beta-amyloid, multimodal analysis

Abbreviations: DTI-ALPS: Diffusion tensor imaging analysis along perivascular space.

Introduction

Brain clearance can be broadly defined as the removal of soluble waste generated from neuronal functioning and other processes via multiple, overlapping systems.[1–8] The glymphatic system is a clearance system in which cerebrospinal fluid (CSF) mixes with interstitial fluid in the perivascular space (PVS) surrounding blood vessels, thereby facilitating the removal of soluble proteins and metabolic wastes from the central nervous system. Glymphatic clearance involves CSF entering the brain along arterial PVS, exchanging with the interstitial fluid, and then exiting along venous PVS. This continuous fluid movement helps to maintain brain health by preventing the accumulation of potentially harmful waste products, such as beta-amyloid (Aβ), a protein associated with Alzheimer's disease (AD).[9,10] Impaired brain CSF clearance causes soluble Aβ accumulation and aggregation into Aβ plaques in the extracellular space, which is one of the hallmarks of AD.[11] It is established that late-onset AD is characterized by an overall impairment in Aβ clearance, not Aβ production. [12] This evidence indicates that an underlying deficit in brain clearance could be a key etiologic mechanism of AD development.

Several neuroimaging methods have been applied to measuring fluid clearance in humans. Using MRI, the rate at which intrathecally injected gadolinium-based contrast travels from a lumbar site of injection to brain PVS can be monitored; this is considered one of the most direct measures of perivascular clearance obtainable in humans, but is inappropriate for routine research use.[13–15] MRI can also track movement of contrast injected intravenously into brain fluid spaces, but this method is hampered by the large size of the gadolinium molecule, which is specifically designed not to enter the brain or its CSF/ISF spaces. Other MRI methods applied to measuring brain fluid movement include Phase contrast MRI (PC-MRI) and functional MRI (fMRI.) PC-MRI quantifies rate, volume and direction of CSF transit through the ventricular system via aqueducts.[16,17] fMRI has been used to assess physiologic low frequency oscillations linked to and driving pulsatile CSF movement through the ventricular system into and out of the brain.[18–23] One of the most promising MR methods is Diffusion Tensor Imaging along perivascular spaces (DTI-ALPS). DTI-ALPS quantifies glymphatic function as diffusivity parallel to PVS surrounding medullary veins. [24,25] DTI-ALPS has demonstrated glymphatic dysfunction in AD [26,27] and other disorders.[28–30] Importantly, glymphatic clearance measured noninvasively using DTI-ALPS has been shown to correlate with a more invasive measure obtained using intrathecal contrast.[24,31]

Dynamic Positron Emission Tomography (PET) is also a promising tool for imaging the glymphatic system.[32–35] We developed a method to measure ventricular CSF clearance/turnover (vCSF) based on the rate of radiotracer removal from lateral ventricle. [33,36] This focus on radiotracer washout differs from the traditional use of PET to assess radiotracer uptake or binding to brain. vCSF can be calculated from dynamic PET using several low weight molecular tracers, and corresponds to the rate of decrease of radiotracer concentration in ventricular CSF normalized by the total amount of tracer delivery. It can also be measured using compartment modeling, which provides convergent results.[37–39] vCSF is a net measure of clearance reflecting several processes critical to clearing the brain solutes: directional flow of CSF (and tracer) within the ventricular system including to subarachnoid space for perivascular/glymphatic clearance; CSF mixing/tracer dilution via pulsatile back-and-forth flow and diffusion within the ventricular system, and tracer dilution via new CSF production (~18–25 ml/h [40]) and diffusion of ISF into ventricle.[8,41,42] We have shown that vCSF is reduced in AD and correlated with Aβ deposition.[7,43]

We hypothesize that DTI-ALPS and vCSF reflect different aspects of the brain CSF clearance. Combining modalities would be expected to provide a more accurate and comprehensive understanding of a complex system involving interconnected brain fluid systems at multiple levels of the nervous system. In addition, showing that independent methods provide convergent information would be important cross validation for both methods as measures of brain clearance in humans given significant controversy in this field. We therefore assessed the ability of two independent noninvasive fluid clearance measures, vCSF and DTI-ALPS, and their combination to predict the extent of cortical Aβ deposition in a large group of well-characterized subjects. Brain Aβ is arguably the only clear-cut evidence in humans of clearance failure and thus appropriate to gauge the relative accuracy of clearance measurement methods.[44,45]

Materials and methods

Subjects

Sixty-nine subjects (age > 50 years) were recruited in this study. All subjects provided informed consent to participate in this IRB approved study. They were recruited by

advertisement or by referral from neurologists. Exclusion criteria includes Exclusions apply to history or MRI evidence of stroke,[46] sleep disorder, probable Cerebral Amyloid Angiopathy (CAA),[47] and severe WM lesions (Fazekas=3);[48] subjects with STAGE 2 hypertension,[49] brain tumors, and other neoplastic disorders outside the brain where disease itself or its treatment (radiation, chemotherapy) is likely to affect brain structure or function. Exclusions are made for lifelong major depression, baseline scores ≥16 on the Hamilton Depression Scale,[50] and lifelong disorders including mental retardation or substance abuse.

Subject assessment

All subjects in this study underwent detailed assessment and evaluation by a cognitive neurologist. The evaluation consisted of neurologic exam, interviews with subject and informant, clinical dementia rating scale (CDR),[51] MOCA[52] and NACC cognitive battery,[53] blood tests and ECG, MRI and amyloid and tau PET examinations. Subjects were assigned a final diagnosis in accord with NACC criteria based on evaluation of all available information. The diagnosis was determined by an experienced neuroradiologist based on ACR criteria. When diagnosis was not straightforward, consensus diagnosis was assigned after discussion at a formal multidisciplinary consensus. Subjects included in this study were diagnosed as either cognitively normal (CN) or with mild cognitive impairment or dementia due to (MCI/AD). Nine subjects missed all required images (MR DTI, 11C-PiB and 18F-MK-6240 PET) were excluded. Four subjects with hydrocephalus,[54] one subject with white matter lesion (Fazekas=3)[48], one subject with sleeping disorder and one subject with microbleeding were excluded. Three subjects diagnosed as MCI and beta amyloid negative (PiB SUVR<1.23) [55] were excluded as well. A chart of participants flow for this study was presented in Figure 1.

PET and MRI acquisition

Subjects underwent MRI on a 3T Siemens Prisma scanner with a 64-channel head-neck coil. T1w used for co-registration and segmentation was acquired using MPRAGE sequence with TR/TE=2400/2.96ms, flip angle=9°, FOV=25.6×25.6cm, matrix size =256×256, 208 sagittal slices, voxel size=0.5x0.5x0.5mm. DTI used for computing DTI-ALPS (PVS clearance)[24] was acquired with 98 directions, TR/TE=3230/89.20ms, flip angle=78°, FOV=21x21cm, matrix size=140x140, voxel size=1.5x1.5x1.5mm, 92 axial slices, 3 b-values=0, 1500, and 3000s/mm2, multiband factor=6. Each DTI scan was acquired with

opposite phase encoding direction for geometric distortion correction. T2w was acquired using T2-SPACE sequence with FOV=256 mm, TR/TE=3200/408ms, matrix size=512x512 with 320 sagittal slices, voxel size=0.5x0.5x0.5 mm3. FLAIR used for WM lesion reading is acquired with 1mm isotropic voxel size, FOV=250 mm, TR/TE=7600/384ms. SWI used for checking micro-bleeding was acquired using multi-echo gradient echo sequence with 10 TEs from 6.1ms to 58.30ms, TR =63ms, FOV=256mm, matrix size=416x512x144, voxel size=0.5x0.5x1 mm3.

PET scanning used a Siemens Biograph mCT–S (64) slice PET/CT. 11C-PiB was synthesized by the Weill Cornell Medicine radiochemistry facility. 18F-MK6240 was provided by the manufacturer. 11C-PiB PET data was acquired from 40-90 min after rapid bolus injection of ~555 MBq. 18F- MK6240 data was acquired from 0-60 min and 90-120 min after rapid bolus injection of ~185 MBq with a break between acquisitions. PiB PET images were reconstructed to a 512 × 512 × 74 matrix of 0.8 × 0.8 × 3 mm voxels in 5 x 10 min time frames from 40min to 90 min. MK6240 PET images were reconstructed to a 400 x 400 x 109 matrix of 1 x 1 x 2 mm voxels with 31 frames (12 x 10 seconds, 3 x 1 min, 10 x 5 min, 6 x 5 min).

Imaging processing

ROI parcellation

T1w MRI was segmented using FreeSurfer1 (FS)[56] version 7.1 recon-all command for ROI parcellation with assistance of T2w to enhance the segmentation quality. ROIs consisted of bilateral cerebellar cortex as a reference region for Aβ SUVr determination, a bilateral parietal, frontal and temporal ROI, referred to as AD cortical mask (ADmask)[57] for quantifying Aβ. All ROIs were eroded one voxel from both sides using 3D sphere kernel to avoid partial volume effect (PVE). The intracranial volume (ICV) was measured using segmented brain mask (GM+WM+CSF) in SPM12.[58]

PiB PET SUVR

Summed PiB PET data from 60 min to 90 min were used for SUVR calculation. All the dynamic frames were realigned to the summed images between 40-90min, and the summed image was then coregistered to the T1w in FS space using boundary-based registration (bbr) method in FS.[59] SUVR was calculated by using the cerebellum cortex as reference. Average

SUVR within the cortical AD mask served as the measure of Aβ deposition.[57] Subjects were classified as quantitatively Aβ positive or negative using a cut-off value SUVR=1.23.[55]

MK6240 vCSF

Dynamic MK6240 data from 0 min to 60 min was used for calculating the brain CSF clearance in lateral ventricle. All the dynamic frames were realigned to the summation of the frames between 6-30 min. The summation was then coregistered to the T1w in FS space using FSL with normalized mutual information (NMI) cost function and the coregistration transformation matrix was saved. Then the transformation matrix was applied to all the dynamic frames to get dynamic MK6240 data in FS space.

The ventricle CSF clearance rate (vCSF) was measured by calculating the slope of the time-activity-curve (TAC) in an ROI consisting of 3-voxels eroded (2D disk kernel) lateral ventricle (LV) during 10min to 30min and normalized by the area under curve (AUC) of the whole brain TAC during 1 min to 4 min. Figure 2 shows the illustrative description of vCSF calculation with formula.

DTI-ALPS

DTI data was corrected for susceptibility-induced geometric and eddy current distortions, and intervolume subject motion using the topup and eddy toolboxes in FSL.[60] The preprocessed dMRI data are used to fit diffusion tensors and obtain fractional anisotropy (FA) and diffusivity maps for each subject in the directions of the x- (right-left, D_{xx}), y- (anterior-posterior, D_{yy}), and z-axes (inferior-superior, D_{zz}). D_{xx} corresponds to the direction of vessels in the periventricular white matter, considered to reflect perivenous water diffusivity and glymphatic function.[24,25] On the color-coded FA map, 5-mm square ROIs are placed bilaterally in the projection and association areas on axial slices at the level of the lateral ventricle body. As shown in Figure 3 (A) the color-coded FA with marked ROIs, and (B) the susceptibility weighted image (SWI) showing medullary veins. Diffusivity values are calculated within each ROI. ALPS-index, reflecting CSF diffusivity in PVS, is calculated as: mean ($D_{xx,proj}$, $D_{xx,assoc}$)/mean($D_{yy,proj}$, $D_{zz,assoc}$).[24,25] Left and right indices are averaged unless quantitative or visual differences e.g. due to lesion/injury are noted.

Statistical analysis

The relationship between Aβ deposition (PiB SUVR within the cortical AD ROI mask) and the clearance measurements (DTI-ALPS and vCSF) was evaluated using multiple regression models controlling for age, sex and ICV. The following regression models were tested (a) vCSF+ALPS model: PiBsuvr = b0 + b1*age + b2*sex + b3*vCSF + b4*ALPS + b5*vCSF*ALPS+b6*ICV; (b) vCSF only model: PiBsuvr = b0 + b1*age + b2*sex + b3*vCSF + b4*ICV and (c) ALPS only model: PiBsuvr = b0 + b1*age + b2*sex + b3*ALPS + b4*ICV. The term of ICV was included in the model to control for head size, which is considered related to the efficiency of brain clearance. And the interaction term between vCSF and ALPS in the vCSF+ALPS model is to account for the interaction between two clearance measures from two different sites and measure mechanisms. This approach will enable us to evaluate if the combination of two clearance measurements could enhance the prediction of Aβ deposits than each individual measurement.

We assessed the whole group of subjects as well as Aβ+ and Aβ- subjects separately. The Akaike information criterion (AIC) and Bayesian information criterion (BIC) of the models were estimated for model comparison. The Pearson correlation between DTI-ALPS and vCSF was evaluated to check the concordance of two clearance measures.

Data availability

Data available upon reasonable request given the need for a formal data sharing agreement between the authors' and the requesting researchers' institutions.

Results

Demographics

Table 1 below shows the demographic and diagnostic information for the subjects in this study.

Table 1. Demographic and clinical information of subjects in this study.

Item	Number

Subjects number (n)	50
Gender: Male	20 (40%)
Mean Age	69.30 (SD=8.55)
Diagnosis	
Cognitive normal	34 (68%)
MCI/AD	16 (32%)
Aβ positive	24 (48%)

Correlation between DTI-ALPS and vCSF

The Pearson correlation between DTI-ALPS and vCSF are r=0.445 (n=50), 0.560 (n=24), 0.311 (n=26) in whole group, Aβ+, and Aβ- groups, respectively.

Prediction of Aβ deposition

For the whole group, in the vCSF-only model, only vCSF was significantly associated with PiB SUVR ($t = -2.221$, $p < 0.05$, $R^2 = 0.174$, AIC = 66.609, BIC = 77.837.) In the ALPS-only model, only ALPS was significantly associated with PiB SUVR ($t = -2.488$, $p < 0.05$, $R^2 = 0.196$, AIC = 65.369, BIC = 76.596.) In the vCSF+ALPS model ($R^2 = 0.286$, AIC = 61.333, BIC = 76.302), vCSF ($t = -2.468$, $p < 0.05$), ALPS ($t = -2.902$, $p<0.05$) and their interaction ($t = 2.334$, $p <0.05$) were all significantly associated with PiB SUVR. The partial regression plots for these significant variables in vCSF+ALPS model are presented in Figure 4.

For the Aβ+ group, in the vCSF-only model, only vCSF was significantly associated with PiB SUVR ($t = -2.885$, $p < 0.05$, $R^2 = 0.431$, AIC = 32.571, BIC = 39.384.) In the ALPS-only model, only ALPS was significantly associated with PiB SUVR ($t = -2.416$, $p < 0.05$, $R^2 = 0.372$, AIC = 34.851, BIC = 41.664.) In the vCSF+ALPS model ($R^2 = 0.575$, AIC = 27.150, BIC = 36.234), vCSF ($t = -2.760$, $p < 0.05$), ALPS ($t = -2.843$, $p < 0.05$) and their interaction ($t = 2.533$, $p < 0.05$) as well as sex ($t = 2.450$, $p < 0.05$) were all significantly associated with PiB SUVR. The partial regression plots for these significant variables in the vCSF+ALPS model are presented in Figure 5.

For the Aβ- group, neither vCSF nor ALPS were significantly associated with PiB SUVR. Only age was significantly associated with the PiB SUVR in ALPS-only model ($p<0.05$, Figure 6 (C)), and marginally associated with PiB SUVR in vCSF-only ($p=0.056$, Figure 6 (B)) and combined ($p=0.053$, Figure 6(A)) models.

Discussion

We found that two independent clearance measures: PET-measured vCSF and MR-measured DTI-ALPS correlated strongly with each other ($r=0.56$ in Aβ+ group), supporting both as in vivo measures of brain fluid clearance. We found that a model including both vCSF, DTI-ALPS and their interaction term (as well as age, sex and ICV) explained a remarkably high proportion of variance in cortical Aβ deposition (57.5%) in Aβ+ subjects. This model explained more variance (higher R^2 and lower AIC and BIC) than either clearance measurement method alone. vCSF and DTI-ALPS are clearance measures measured using different mechanisms and from different brain sites. That two independent clearance measures correlate strongly with each other and with cortical amyloid – the only available gold standard measure of prior failed clearance - strongly support their validity as in vivo clearance measures. At the same time, the fact that both DTI-ALPS and vCSF contribute independently to explaining variability in Aβ deposition indicates that they reflect different aspects of fluid clearance and provide complementary information relevant to Aβ deposition and clearance.

The explanatory power increased dramatically for the Aβ+ group (57.5%) compared with the whole group consisting of Aβ+ and Aβ- subjects (only 28.6%.) In Aβ- subjects (Figure 4) neither clearance measure explained cortical Aβ. These results make sense when considering that in subjects with significant, above-threshold Aβ accumulation, a clear-cut inverse relation between clearance and Aβ is expected (i.e., worse clearance = higher Aβ). In contrast, in Aβ- subjects, the relation between clearance and Aβ may be more complex, with clearance rates likely homeostatically linked to Aβ production/deposition in some but not all subjects. In addition, the very limited range of Aβ load in Aβ- subjects would make detection of clearance- Aβ correlations difficult.

Glymphatic clearance depends on interconnected fluid systems including the recently characterized glymphatic system involving convective exchange of CSF and ISF through PVS

and the traditional, well-studied traditional CSF system consisting of ventricles and connecting aqueducts. The interrelationship between bulk CSF flow and glymphatic flow has been widely discussed.[61–63] Breakdown at any point within these interconnected systems may reduce CSF-ISF flow/mixing and impair clearance, including clearance of Aβ, leading to its accumulation. Our data showed both glymphatic function (DTI-ALPS) and ventricular CSF clearance/turnover (VCSF) are highly relevant to brain Aβ deposition. The ability to measure and monitor brain clearance in vivo in humans is expected to inform understanding of AD pathogenesis and guide targeted therapies.

Conclusion

Our results show that two independent brain clearance measurements - MRI-measured DTI-ALPS and PET-measured vCSF - correlate strongly with each other, and a regression model including both measures predicts Aβ deposition more accurately than either method alone. These results indicate that vCSF and ALPS reflect different and complementary aspects of the brain clearance in humans. Reliable methods for measuring clearance in humans are essential to understanding how clearance failure may lead to AD, for identifying reduced clearance in asymptomatic subjects potentially at risk of neurodegeneration, and for testing the effectiveness of interventions designed to boost clearance and prevent disease.

Author contributions

LZ, TB, and YL: conceptualization. TB, and YL: study design. LZ, XH, and YL: imaging and data processing. LZ, KX and LG: analysis and statistics. LZ, TB, and YL: original draft. LZ, TB, XW, KX, ET, LG, GC, ML and TL: review and editing. All authors contributed to the article and approved the submitted version.

Funding

This work was conducted with grants supported by NIH (R01 R56AG058913, R01 AG068398, AG057848, R01AG022374, RF1 AG057570).

Competing interests

The authors report no competing interests.

References

1. Hladky SB, Barrand MA. Elimination of substances from the brain parenchyma: efflux via perivascular pathways and via the blood–brain barrier. *Fluids and Barriers of the CNS*. 2018;15(1):30. doi:10.1186/s12987-018-0113-6

2. Abbott NJ, Pizzo ME, Preston JE, Janigro D, Thorne RG. The role of brain barriers in fluid movement in the CNS: is there a "glymphatic" system? *Acta Neuropathol*. 2018;135(3):387-407. doi:10.1007/s00401-018-1812-4

3. Bakker ENTP, Bacskai BJ, Arbel-Ornath M, et al. Lymphatic Clearance of the Brain: Perivascular, Paravascular and Significance for Neurodegenerative Diseases. *Cell Mol Neurobiol*. 2016;36(2):181-194. doi:10.1007/s10571-015-0273-8

4. Louveau A, Plog BA, Antila S, Alitalo K, Nedergaard M, Kipnis J. Understanding the functions and relationships of the glymphatic system and meningeal lymphatics. *J Clin Invest*. 2017;127(9):3210-3219. doi:10.1172/JCI90603

5. Mestre H, Mori Y, Nedergaard M. The Brain's Glymphatic System: Current Controversies. *Trends Neurosci*. 2020;43(7):458-466. doi:10.1016/j.tins.2020.04.003

6. Benveniste H, Liu X, Koundal S, Sanggaard S, Lee H, Wardlaw J. The Glymphatic System and Waste Clearance with Brain Aging: A Review. *GER*. 2019;65(2):106-119. doi:10.1159/000490349

7. de Leon MJ, Li Y, Okamura N, et al. Cerebrospinal Fluid Clearance in Alzheimer Disease Measured with Dynamic PET. *J Nucl Med*. 2017;58(9):1471-1476. doi:10.2967/jnumed.116.187211

8. Syková E, Nicholson C. Diffusion in Brain Extracellular Space. *Physiol Rev*. 2008;88(4):1277-1340. doi:10.1152/physrev.00027.2007

9. Iliff JJ, Wang M, Liao Y, et al. A Paravascular Pathway Facilitates CSF Flow Through the Brain Parenchyma and the Clearance of Interstitial Solutes, Including Amyloid β. *Science Translational Medicine*. 2012;4(147):147ra111-147ra111. doi:10.1126/scitranslmed.3003748

10. Jessen NA, Munk ASF, Lundgaard I, Nedergaard M. The Glymphatic System – A Beginner's Guide. *Neurochem Res*. 2015;40(12):2583-2599. doi:10.1007/s11064-015-1581-6

11. Tarasoff-Conway JM, Carare RO, Osorio RS, et al. Clearance systems in the brain-implications for Alzheimer disease. *Nat Rev Neurol*. 2015;11(8):457-470. doi:10.1038/nrneurol.2015.119

12. Mawuenyega KG, Sigurdson W, Ovod V, et al. Decreased clearance of CNS beta-amyloid in Alzheimer's disease. *Science*. 2010;330(6012):1774. doi:10.1126/science.1197623

13. Eide PK, Valnes LM, Lindstrøm EK, Mardal KA, Ringstad G. Direction and magnitude of cerebrospinal fluid flow vary substantially across central nervous system diseases. *Fluids and Barriers of the CNS*. 2021;18(1):16. doi:10.1186/s12987-021-00251-6

14. Eide PK, Vinje V, Pripp AH, Mardal KA, Ringstad G. Sleep deprivation impairs molecular clearance from the human brain. *Brain*. 2021;144(3):863-874. doi:10.1093/brain/awaa443

15. Ringstad G, Vatnehol SAS, Eide PK. Glymphatic MRI in idiopathic normal pressure hydrocephalus. *Brain*. 2017;140(10):2691-2705. doi:10.1093/brain/awx191

16. Sakhare AR, Barisano G, Pa J. Assessing test-retest reliability of phase contrast MRI for measuring cerebrospinal fluid and cerebral blood flow dynamics. *Magn Reson Med*. 2019;82(2):658-670. doi:10.1002/mrm.27752

17. El Sankari S, Gondry-Jouet C, Fichten A, et al. Cerebrospinal fluid and blood flow in mild cognitive impairment and Alzheimer's disease: a differential diagnosis from idiopathic normal pressure hydrocephalus. *Fluids Barriers CNS*. 2011;8(1):12. doi:10.1186/2045-8118-8-12

18. Han F, Brown GL, Zhu Y, et al. Decoupling of Global Brain Activity and Cerebrospinal Fluid Flow in Parkinson's Disease Cognitive Decline. *Mov Disord*. 2021;36(9):2066-2076. doi:10.1002/mds.28643

19. Kiviniemi V, Wang X, Korhonen V, et al. Ultra-fast magnetic resonance encephalography of physiological brain activity - Glymphatic pulsation mechanisms? *J Cereb Blood Flow Metab*. 2016;36(6):1033-1045. doi:10.1177/0271678X15622047

20. Fultz NE, Bonmassar G, Setsompop K, et al. Coupled electrophysiological, hemodynamic, and cerebrospinal fluid oscillations in human sleep. *Science*. 2019;366(6465):628-631. doi:10.1126/science.aax5440

21. Yang HC (Shawn), Inglis B, Talavage T, et al. Coupling brain cerebrovascular oscillations and CSF flow during wakefulness: An fMRI study. *bioRxiv*. Published online March 30, 2021:2021.03.29.437406. doi:10.1101/2021.03.29.437406

22. Gonzalez-Castillo J, Fernandez IS, Handwerker DA, Bandettini PA. Ultra-slow fMRI fluctuations in the fourth ventricle as a marker of drowsiness. *Neuroimage*. 2022;259:119424. doi:10.1016/j.neuroimage.2022.119424

23. Han F, Chen J, Belkin-Rosen A, et al. Reduced coupling between cerebrospinal fluid flow and global brain activity is linked to Alzheimer disease–related pathology. *PLOS Biology*. 2021;19(6):e3001233. doi:10.1371/journal.pbio.3001233

24. Taoka T, Masutani Y, Kawai H, et al. Evaluation of glymphatic system activity with the diffusion MR technique: diffusion tensor image analysis along the perivascular space (DTI-

ALPS) in Alzheimer's disease cases. *Jpn J Radiol*. 2017;35(4):172-178. doi:10.1007/s11604-017-0617-z

25. Taoka T, Ito R, Nakamichi R, et al. Reproducibility of diffusion tensor image analysis along the perivascular space (DTI-ALPS) for evaluating interstitial fluid diffusivity and glymphatic function: CHanges in Alps index on Multiple conditiON acquIsition eXperiment (CHAMONIX) study. *Jpn J Radiol*. 2022;40(2):147-158. doi:10.1007/s11604-021-01187-5

26. Hsu JL, Wei YC, Toh CH, et al. Magnetic Resonance Images Implicate That Glymphatic Alterations Mediate Cognitive Dysfunction in Alzheimer Disease. *Ann Neurol*. 2023;93(1):164-174. doi:10.1002/ana.26516

27. Kamagata K, Andica C, Takabayashi K, et al. Association of MRI Indices of Glymphatic System With Amyloid Deposition and Cognition in Mild Cognitive Impairment and Alzheimer Disease. *Neurology*. 2022;99(24):e2648-e2660. doi:10.1212/WNL.0000000000201300

28. McKnight CD, Trujillo P, Lopez AM, et al. Diffusion along perivascular spaces reveals evidence supportive of glymphatic function impairment in Parkinson disease. *Parkinsonism Relat Disord*. 2021;89:98-104. doi:10.1016/j.parkreldis.2021.06.004

29. Si X, Guo T, Wang Z, et al. Neuroimaging evidence of glymphatic system dysfunction in possible REM sleep behavior disorder and Parkinson's disease. *npj Parkinsons Dis*. 2022;8(1):1-9. doi:10.1038/s41531-022-00316-9

30. Carotenuto A, Cacciaguerra L, Pagani E, Preziosa P, Filippi M, Rocca MA. Glymphatic system impairment in multiple sclerosis: relation with brain damage and disability. *Brain*. 2022;145(8):2785-2795. doi:10.1093/brain/awab454

31. Yokota H, Vijayasarathi A, Cekic M, et al. Diagnostic Performance of Glymphatic System Evaluation Using Diffusion Tensor Imaging in Idiopathic Normal Pressure Hydrocephalus and Mimickers. *Curr Gerontol Geriatr Res*. 2019;2019:5675014. doi:10.1155/2019/5675014

32. Sigurdsson B, Hauglund NL, Lilius TO, et al. A SPECT-based method for dynamic imaging of the glymphatic system in rats. *J Cereb Blood Flow Metab*. Published online February 21, 2023:271678X231156982. doi:10.1177/0271678X231156982

33. de Leon MJ, Li Y, Okamura N, et al. Cerebrospinal fluid clearance in Alzheimer Disease measured with dynamic PET. *JNuclMed*. 2017;58(9):1471-1476. doi:10.2967/jnumed.116.187211

34. Schubert JJ, Veronese M, Marchitelli L, et al. Dynamic 11C-PIB PET shows cerebrospinal fluid flow alterations in Alzheimer disease and multiple sclerosis. *Journal of Nuclear Medicine*. 2019;60(10):1452-1460.

35. Turkheimer FE, Althubaity N, Schubert J, et al. Increased serum peripheral C-reactive protein is associated with reduced brain barriers permeability of TSPO radioligands in healthy volunteers and depressed patients: implications for inflammation and depression. *Brain Behav Immun*. 2021;91:487-497. doi:10.1016/j.bbi.2020.10.025

36. li yi, Rusinek H, Butler T, et al. Decreased CSF clearance and increased brain amyloid in Alzheimer's disease. Published online October 13, 2021. doi:10.21203/rs.3.rs-900478/v1

37. Schubert JJ, Veronese M, Marchitelli L, et al. Dynamic 11C-PiB PET Shows Cerebrospinal Fluid Flow Alterations in Alzheimer Disease and Multiple Sclerosis. *J Nucl Med*. 2019;60(10):1452-1460. doi:10.2967/jnumed.118.223834

38. Turkheimer FE, Althubaity N, Schubert J, et al. Increased serum peripheral C-reactive protein is associated with reduced brain barriers permeability of TSPO radioligands in healthy volunteers and depressed patients: implications for inflammation and depression. *Brain Behav Immun*. 2021;91:487-497. doi:10.1016/j.bbi.2020.10.025

39. Althubaity N, Schubert J, Martins D, et al. Choroid plexus enlargement is associated with neuroinflammation and reduction of blood brain barrier permeability in depression. *Neuroimage Clin*. 2022;33:102926. doi:10.1016/j.nicl.2021.102926

40. Brown PD, Davies SL, Speake T, Millar ID. Molecular mechanisms of cerebrospinal fluid production. *Neuroscience*. 2004;129(4):957-970. doi:10.1016/j.neuroscience.2004.07.003

41. Pathways of Fluid Drainage from the Brain - Morphological Aspects and Immunological Significance in Rat and Man - Weller - 1992 - Brain Pathology - Wiley Online Library. Accessed February 9, 2023. https://onlinelibrary.wiley.com/doi/10.1111/j.1750-3639.1992.tb00704.x

42. Bedussi B, van Lier MGJTB, Bartstra JW, et al. Clearance from the mouse brain by convection of interstitial fluid towards the ventricular system. *Fluids Barriers CNS*. 2015;12:23. doi:10.1186/s12987-015-0019-5

43. Li Y, Rusinek H, Butler T, et al. Decreased CSF clearance and increased brain amyloid in Alzheimer's disease. *Fluids and Barriers of the CNS*. 2022;19(1):21. doi:10.1186/s12987-022-00318-y

44. Fagan AM, Mintun MA, Mach RH, et al. Inverse relation between in vivo amyloid imaging load and cerebrospinal fluid Abeta42 in humans. *Ann Neurol*. 2006;59(3):512-519. doi:10.1002/ana.20730

45. McLean CA, Cherny RA, Fraser FW, et al. Soluble pool of Abeta amyloid as a determinant of severity of neurodegeneration in Alzheimer's disease. *Ann Neurol*. 1999;46(6):860-866. doi:10.1002/1531-8249(199912)46:6<860::aid-ana8>3.0.co;2-m

46. Bamford J, Sandercock P, Dennis M, Warlow C, Burn J. Classification and natural history of clinically identifiable subtypes of cerebral infarction. *Lancet*. 1991;337(Journal Article):1521-1526.

47. Greenberg SM, Charidimou A. Diagnosis of Cerebral Amyloid Angiopathy. *Stroke*. 2018;49(2):491-497. doi:10.1161/STROKEAHA.117.016990

48. Fazekas F, Chawluk JB, Alavi A, Hurtig HI, Zimmerman RA. MR signal abnormalities at 1.5 T in Alzheimer's dementia and normal aging. *AJR Am J Roentgenol*. 1987;149(2):351-356. doi:10.2214/ajr.149.2.351

49. Chobanian AV, Bakris GL, Black HR, et al. Seventh report of the Joint National Committee on Prevention, Detection, Evaluation, and Treatment of High Blood Pressure. *Hypertension*. 2003;42(6):1206-1252. doi:10.1161/01.HYP.0000107251.49515.c2

50. Hamilton M. A rating scale for depression. *J Neurol Neurosurg Psychiatry*. 1960;23(1):56-62. doi:10.1136/jnnp.23.1.56

51. Morris JC. The Clinical Dementia Rating (CDR): Current version and scoring rules. *Neurology*. 1993;43(11):2412-a. doi:10.1212/WNL.43.11.2412-a

52. Nasreddine ZS, Phillips NA, Bédirian V, et al. The Montreal Cognitive Assessment, MoCA: A Brief Screening Tool For Mild Cognitive Impairment. *Journal of the American Geriatrics Society*. 2005;53(4):695-699. doi:10.1111/j.1532-5415.2005.53221.x

53. Besser L, Kukull W, Knopman DS, et al. Version 3 of the National Alzheimer's Coordinating Center's Uniform Data Set. *Alzheimer Dis Assoc Disord*. 2018;32(4):351-358. doi:10.1097/WAD.0000000000000279

54. Evans WA Jr. An encephalographic ratio for estimating ventricular enlargement and cerebral atrophy. *Archives of Neurology & Psychiatry*. 1942;47(6):931-937. doi:10.1001/archneurpsyc.1942.02290060069004

55. Villeneuve S, Rabinovici GD, Cohn-Sheehy BI, et al. Existing Pittsburgh Compound-B positron emission tomography thresholds are too high: statistical and pathological evaluation. *Brain*. 2015;138(7):2020-2033. doi:10.1093/brain/awv112

56. Fischl B. FreeSurfer. *Neuroimage*. 2012;62(2):774-781. doi:10.1016/j.neuroimage.2012.01.021

57. Mosconi L, Rinne JO, Tsui WH, et al. Increased fibrillar amyloid-β burden in normal individuals with a family history of late-onset Alzheimer's. *Proc Natl Acad Sci U S A*. 2010;107(13):5949-5954. doi:10.1073/pnas.0914141107

58. Ashburner J, Friston KJ. Unified segmentation. *Neuroimage*. 2005;26(3):839-851. doi:10.1016/j.neuroimage.2005.02.018

59. Accurate and robust brain image alignment using boundary-based registration - PubMed. Accessed February 10, 2023. https://pubmed.ncbi.nlm.nih.gov/19573611/

60. Andersson JLR, Sotiropoulos SN. An integrated approach to correction for off-resonance effects and subject movement in diffusion MR imaging. *Neuroimage*. 2016;125:1063-1078. doi:10.1016/j.neuroimage.2015.10.019

61. Jessen NA, Munk ASF, Lundgaard I, Nedergaard M. The Glymphatic System – A Beginner's Guide. *Neurochem Res*. 2015;40(12):2583-2599. doi:10.1007/s11064-015-1581-6

62. Schubert JJ, Veronese M, Marchitelli L, et al. Dynamic 11C-PiB PET Shows Cerebrospinal Fluid Flow Alterations in Alzheimer Disease and Multiple Sclerosis. *J Nucl Med*. 2019;60(10):1452-1460. doi:10.2967/jnumed.118.223834

63. Akins PT, Guppy KH. Does Impaired Glymphatic Drainage Cause Glymphedema? A Review Tailored to Neurocritical Care and Neurosurgery. *Neurocrit Care*. Published online June 10, 2021. doi:10.1007/s12028-021-01224-1

Figure legends

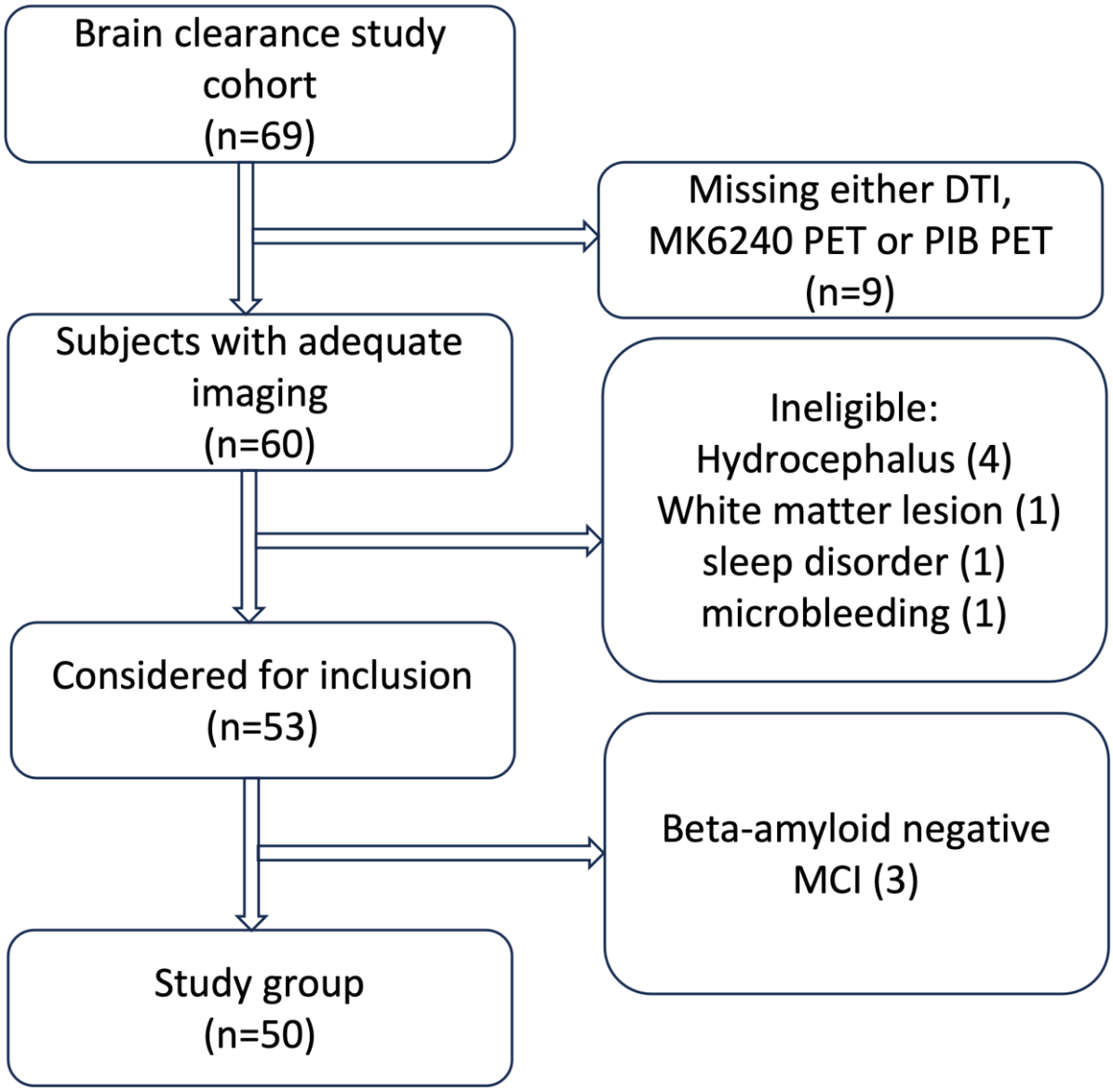

Figure 1 Flowchart of participants finalization.

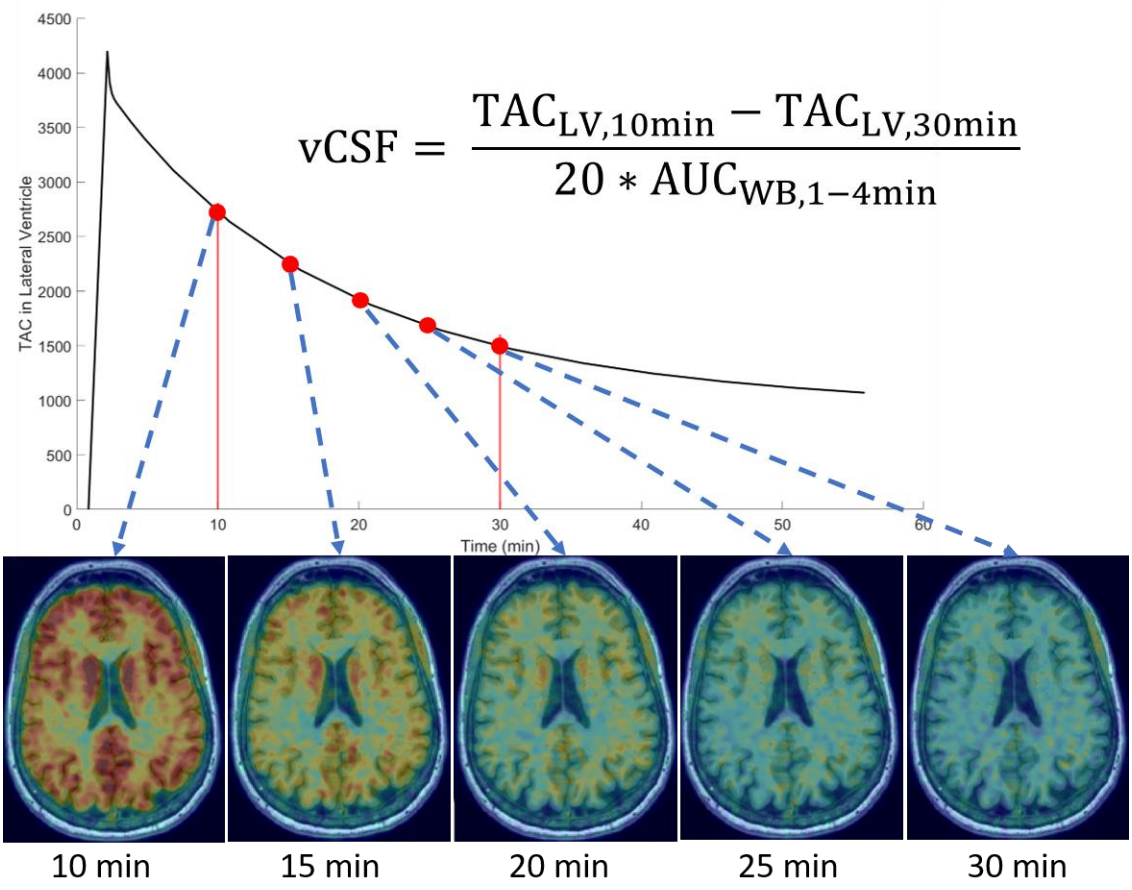

Figure 2 Illustration of dynamic 18F-MK6240 in the brain and formulation for calculation of vCSF using TAC in lateral ventricle and area under curve (AUC) of whole brain (WB) TAC.

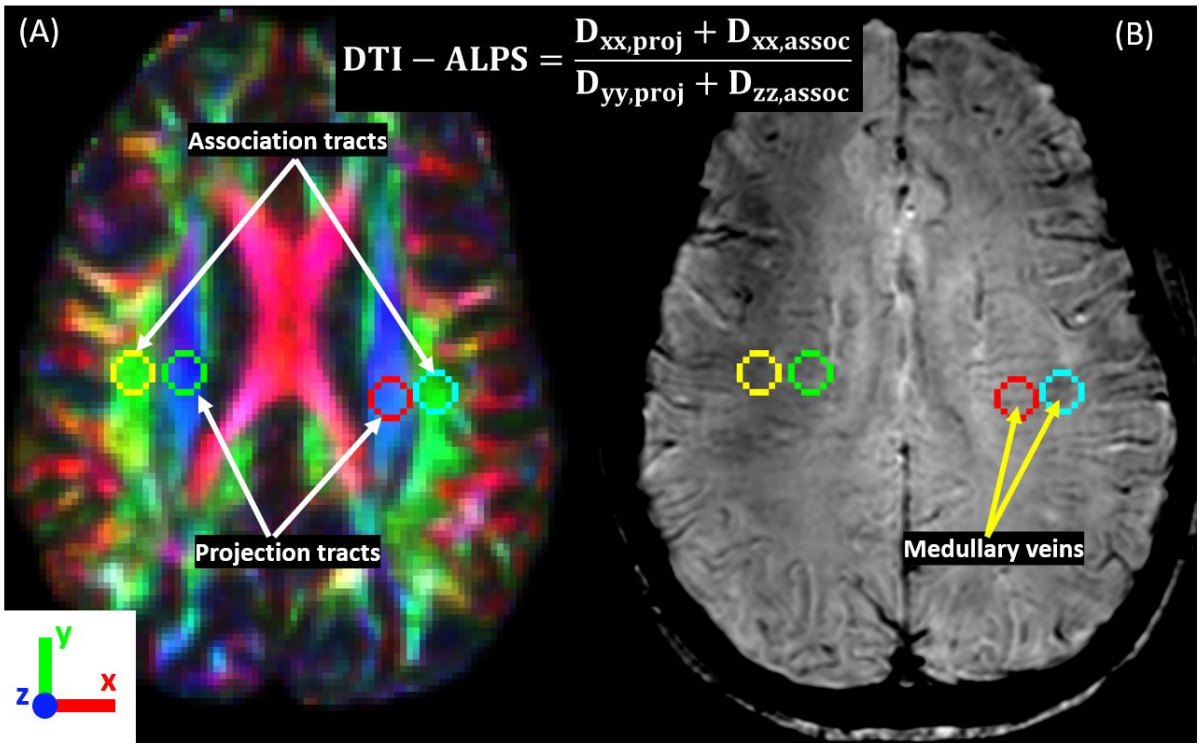

Figure 3 Illustration of ROIs on (A) color-coded FA for DTI-ALPS, white matter fiber directions and (B) the medullary veins on SWI.

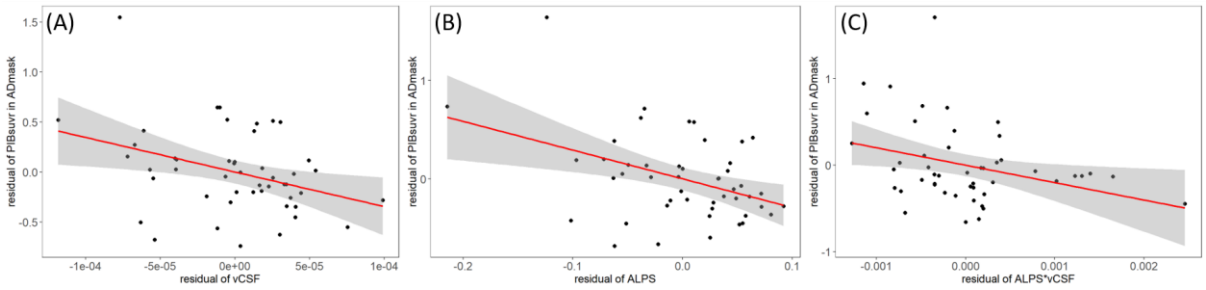

Figure 4 In whole group, partial regression plot of significant variables versus Aβ deposit in AD mask in vCSF+ALPS model. (A) vCSF; (B) ALPS; and (C) ALPS*vCSF.

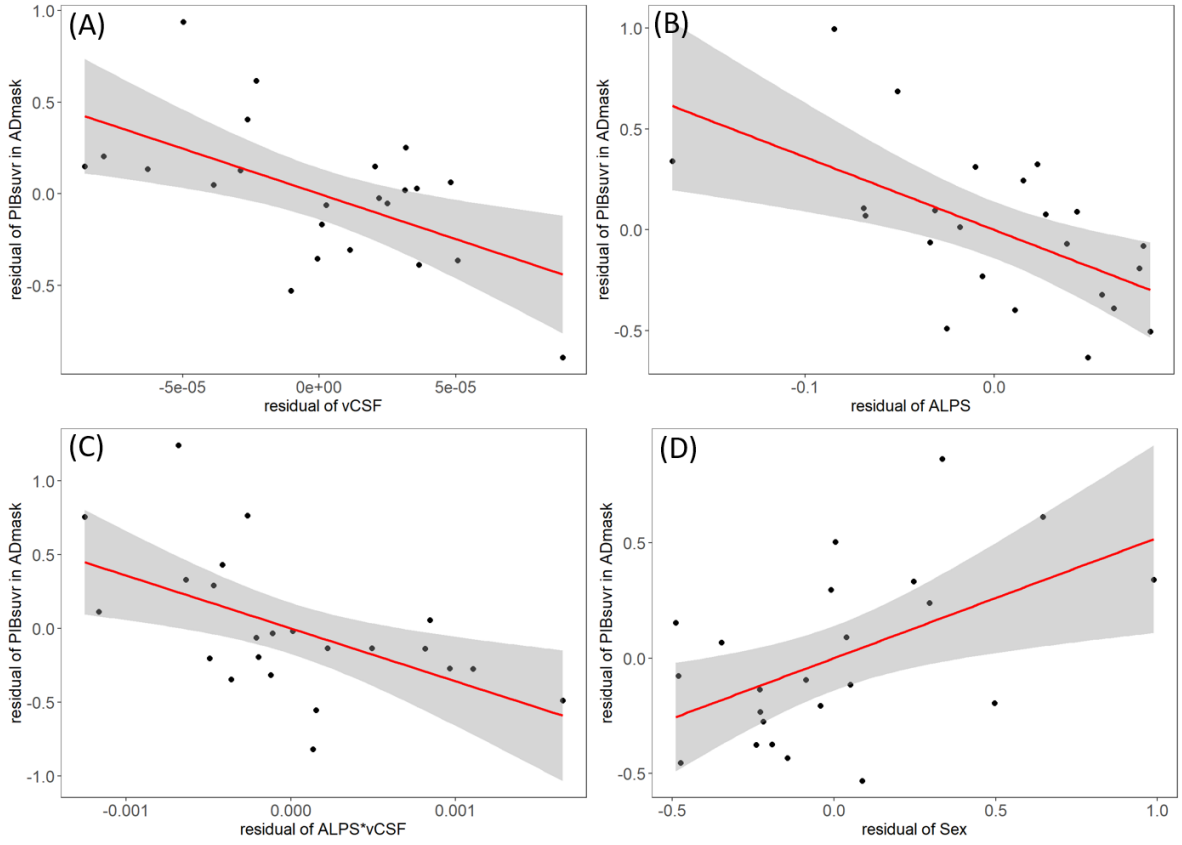

Figure 5 In Aβ positive group, partial regression plot of significant variables versus Aβ deposit in AD mask in vCSF+ALPS model. (A) vCSF; (B) ALPS; (C) ALPS*vCSF; and (D) Sex.

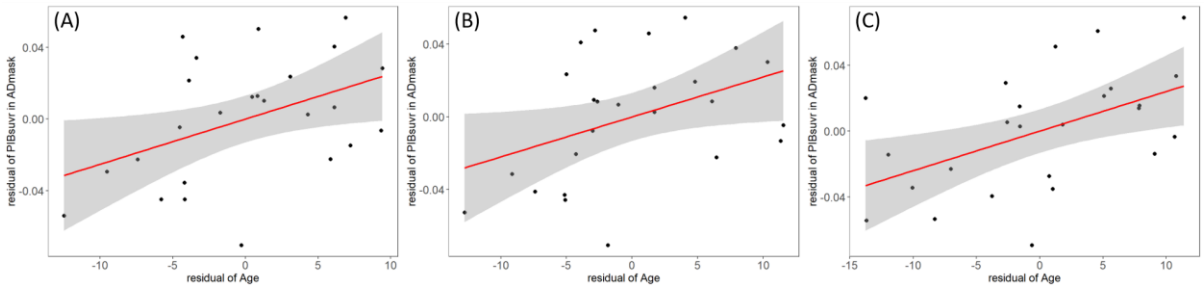

Figure 6 In Aβ negative group, partial regression plot of significant variable (Age) versus Aβ deposit measured in AD mask in (A) vCSF+ALPS model, (B) vCSF model; and (C) ALPS model.

Author responsibilities, integrity, ethics

This is an **editable** PDF form. It should **be saved to your computer, then completed** using Adobe reader or equivalent. Please **do NOT substitute** any other document (text file, scanned image, etc.).

Article title : Multimodal Assessment of Brain Fluid Clearance Predicts Amyloid-beta Deposition in Humans

Human and animal rights

☑ The authors declare that the work described has been carried out in accordance with the Declaration of Helsinki of the World Medical Association revised in 2013 for experiments involving humans as well as in accordance with the EU Directive 2010/63/EU for animal experiments.

☐ The authors declare that the work described has not involved experimentation on humans or animals.

Informed consent and patient details

☐ The authors declare that this report does not contain any personal information that could lead to the identification of the patient(s) and/or volunteers.

☑ The authors declare that they obtained a written informed consent from the patients and/or volunteers included in the article and that this report does not contain any personal information that could lead to their identification.

☐ The authors declare that the work described does not involve patients or volunteers.

Disclosure of interest

☑ The authors declare that they have no known competing financial or personal relationships that could be viewed as influencing the work reported in this paper.

☐ The authors declare the following financial or personal relationships that could be viewed as influencing the work reported in this paper:

Funding

☐ This work did not receive any grant from funding agencies in the public, commercial, or not-for-profit sectors.

☑ This work has been supported by:

NIH (R01 R56AG058913, R01 AG068398, AG057848, R01AG022374, RF1 AG057570)

Author contributions

☑ All authors attest that they meet the current International Committee of Medical Journal Editors (ICMJE) criteria for Authorship.

☐ All authors attest that they meet the current International Committee of Medical Journal Editors (ICMJE) criteria for Authorship. Individual author contributions are as follows:

Figure 6

Click here to access/download;Figure;Figure 6.png

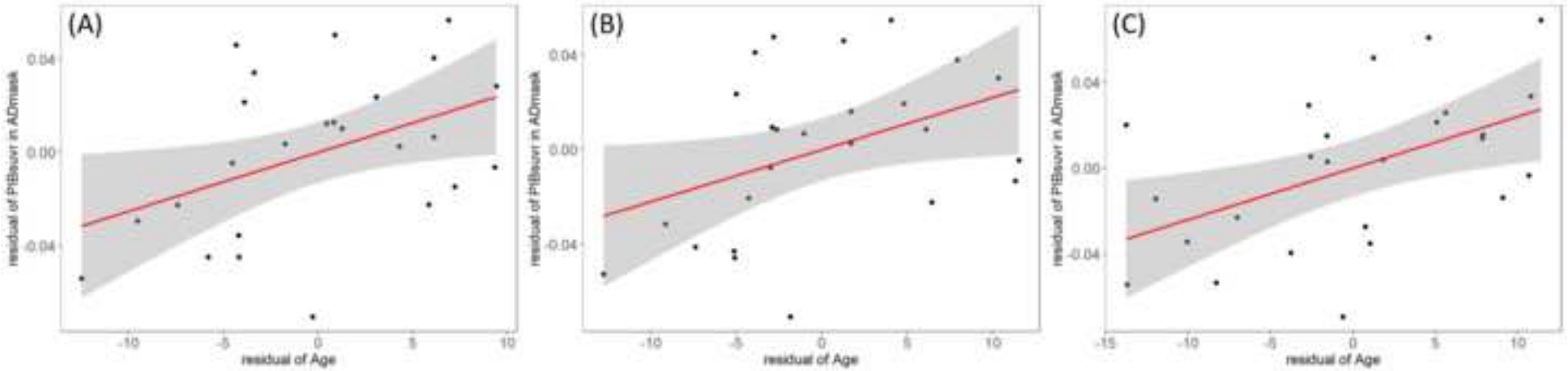

Figure 1

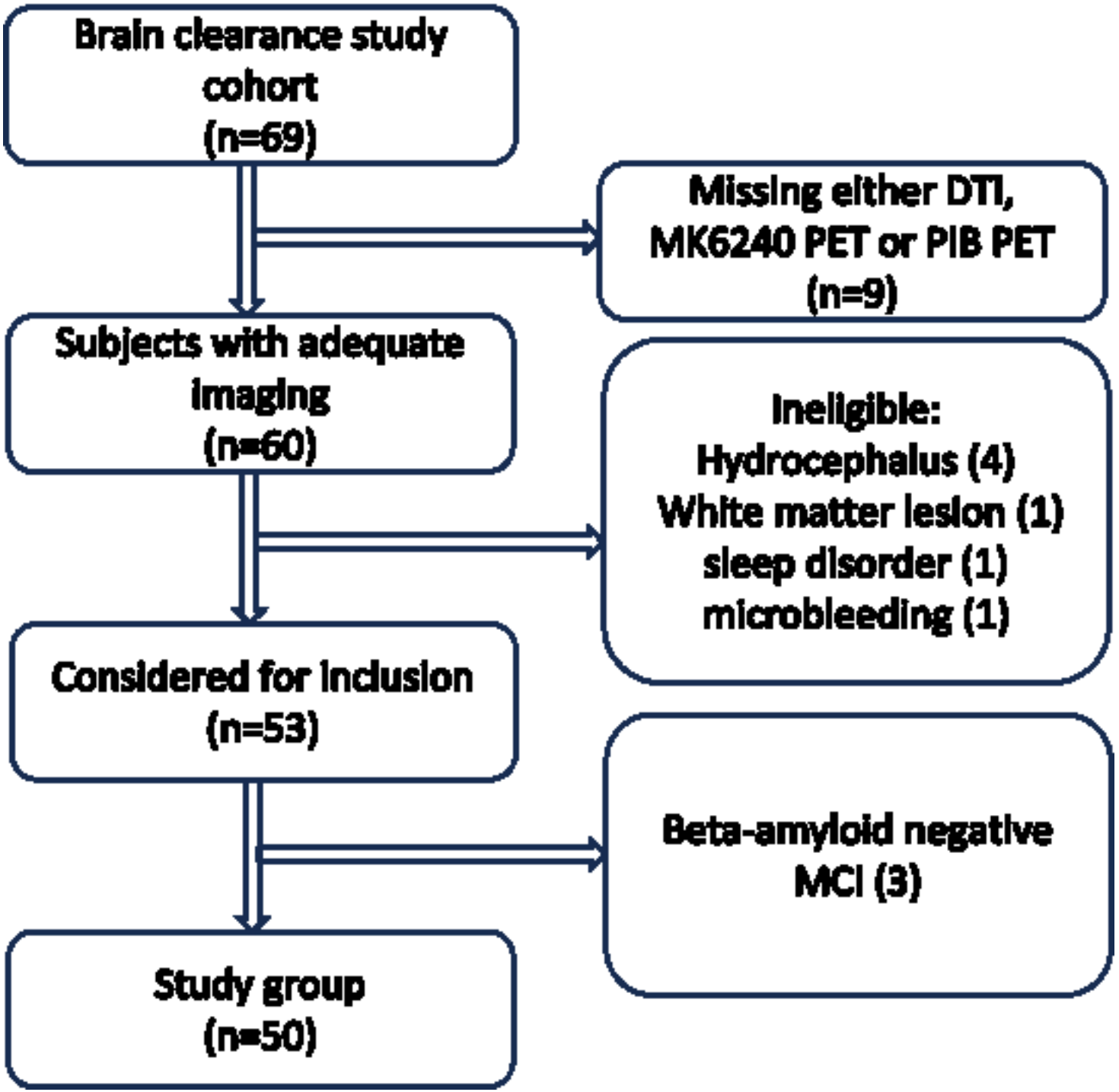

Figure 2

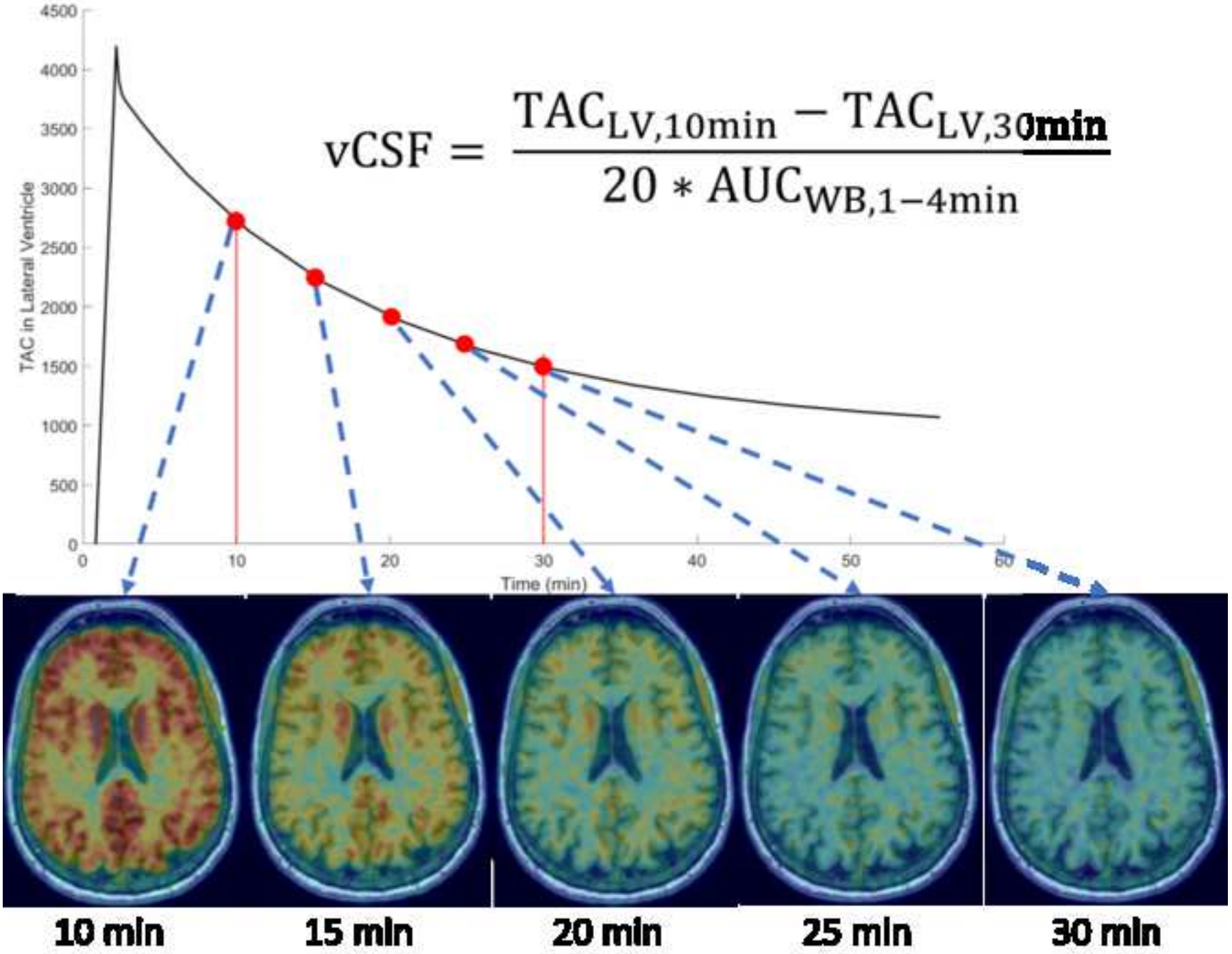

Figure 3

Click here to access/download;Figure;Figure 3.png

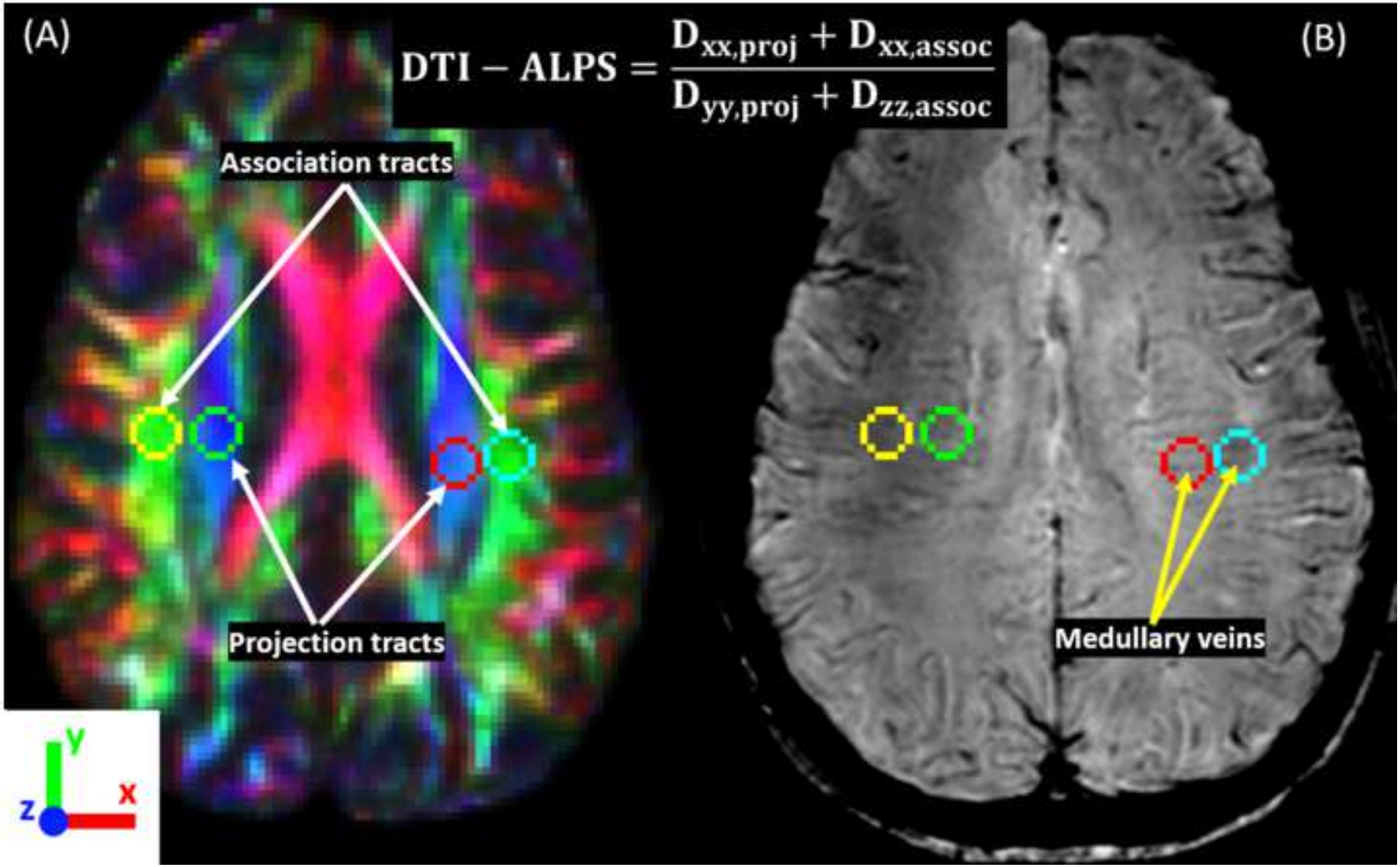

Figure 4

Click here to access/download;Figure;Figure 4.png

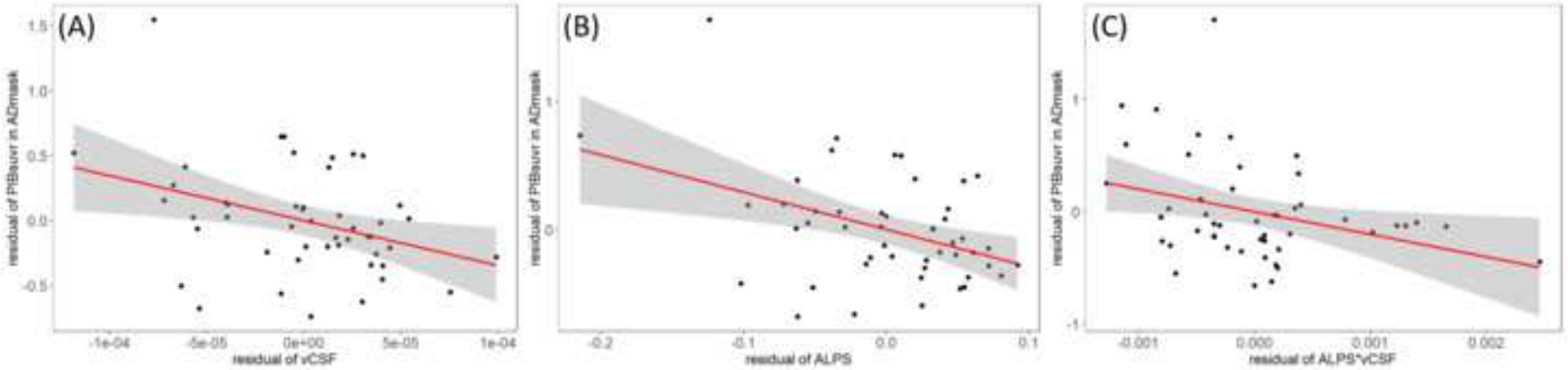

Figure 5

Click here to access/download;Figure;Figure 5.png